Stem Cell Reports
Article

ISSCR

OPEN ACCESS

Piwi maintains homeostasis in the *Drosophila* adult intestine

Xiongzhuo Tang,[1,2,*] Na Liu,[1,2] Hongying Qi,[1,2] and Haifan Lin[1,2,*]
[1]Yale Stem Cell Center, Yale School of Medicine, New Haven, CT 06519, USA
[2]Department of Cell Biology, Yale School of Medicine, New Haven, CT 06519, USA
*Correspondence: xiongzhuo.tang@yale.edu (X.T.), haifan.lin@yale.edu (H.L.)
https://doi.org/10.1016/j.stemcr.2023.01.001

ASSOCIATED PODCAST For an associated discussion of this work, listen to the latest episode of *The Stem Cell Report* podcast at https://www.isscr.org/podcast/s2-e7, brought to you by the ISSCR.

SUMMARY

PIWI genes are well known for their germline but not somatic functions. Here, we report the function of the *Drosophila piwi* gene in the adult gut, where intestinal stem cells (ISCs) produce enteroendocrine cells and enteroblasts that generate enterocytes. We show that *piwi* is expressed in ISCs and enteroblasts. *Piwi* deficiency reduced ISC number, compromised enteroblasts maintenance, and induced apoptosis in enterocytes, but did not affect ISC proliferation and its differentiation to enteroendocrine cells. In addition, deficiency of zygotic but not maternal *piwi* mildly de-silenced several retrotransposons in the adult gut. Importantly, either *piwi* mutations or *piwi* knockdown specifically in ISCs and enteroblasts shortened the *Drosophila* lifespan, indicating that intestinal *piwi* contributes to longevity. Finally, our mRNA sequencing data implied that Piwi may achieve its intestinal function by regulating diverse molecular processes involved in metabolism and oxidation-reduction reaction.

INTRODUCTION

The epithelium is maintained by epithelial stem cells that undergo constant self-renewing divisions to replenish various types of damaged and lost epithelial cells. Epithelial stem cell function is regulated by both intrinsic and extrinsic mechanisms. The *Drosophila* midgut provides a genetically amenable model for studying these mechanisms (Lemaitre and Miguel-Aliaga, 2013).

The *Drosophila* midgut is composed of a monolayer of epithelial cells that rest on a thin layer of muscle cells. This epithelium shares high anatomic and functional similarities with the mammalian small intestine (Apidianakis and Rahme, 2011). In the *Drosophila* intestinal epithelium, the bipotent intestinal stem cells (ISCs) produce the hormone-secreting enteroendocrine cells (EEs) lineage and the absorptive lineage that contains a small number of enteroblasts (EBs) and a large number of their differentiated daughter cells—enterocytes (ECs) (Micchelli and Perrimon, 2006; Ohlstein and Spradling, 2006). The four types of intestinal cells can be experimentally marked and tracked by using well-developed *Drosophila* genetic tools (Micchelli and Perrimon, 2006; Ohlstein and Spradling, 2006). Both ISCs and EBs express the Escargot (Esg) transcription factor but EBs also express the Notch transactivation reporter Su(H)GBE (Furriols and Bray, 2001), whereas EEs express the Prospero transcription factor. Similar to other stem cell systems, the self-renewal and differentiation of ISCs are controlled by a complex regulatory network to maintain tissue homeostasis.

The PAZ/PIWI Domain protein family consists of the Argonaute (AGO) and the PIWI subfamilies, both of which regulate gene expression by associating with small noncoding RNAs. In *Drosophila*, the AGO subfamily proteins Ago1 and Ago2 associate with microRNA (miRNA) and small interfering RNA (siRNA), respectively, whereas the PIWI subfamily proteins Piwi, Aubergine (Aub), and Ago3 bind to PIWI-interacting RNAs (piRNAs) (Ross et al., 2014). Herein we use PIWI to denote the subfamily and Piwi to denote the *Drosophila piwi* gene product. A well-known function of the PIWI-piRNA pathway is transposable element (TE) silencing, which occurs at both transcriptional and post-transcriptional levels. In the nucleus, Piwi acts together with other mediator proteins (e.g., Panoramix/Silencio, Nxf1/3, Nxt1) to suppress TE transcription by introducing repressive epigenetic marks at their target sites (Yu et al., 2015; Sienski et al., 2015; El-Maghraby et al., 2019). Meanwhile in the cytoplasm, Aub and Ago3 restrict TE expression by degrading TE mRNAs and/or inhibiting their translation (Yamashiro and Siomi, 2018; Ramat and Simonelig, 2021). In both mechanisms, piRNAs play critical roles in directing the PIWI/piRNA complex to its target sites via base-pairing to ensure target specificity.

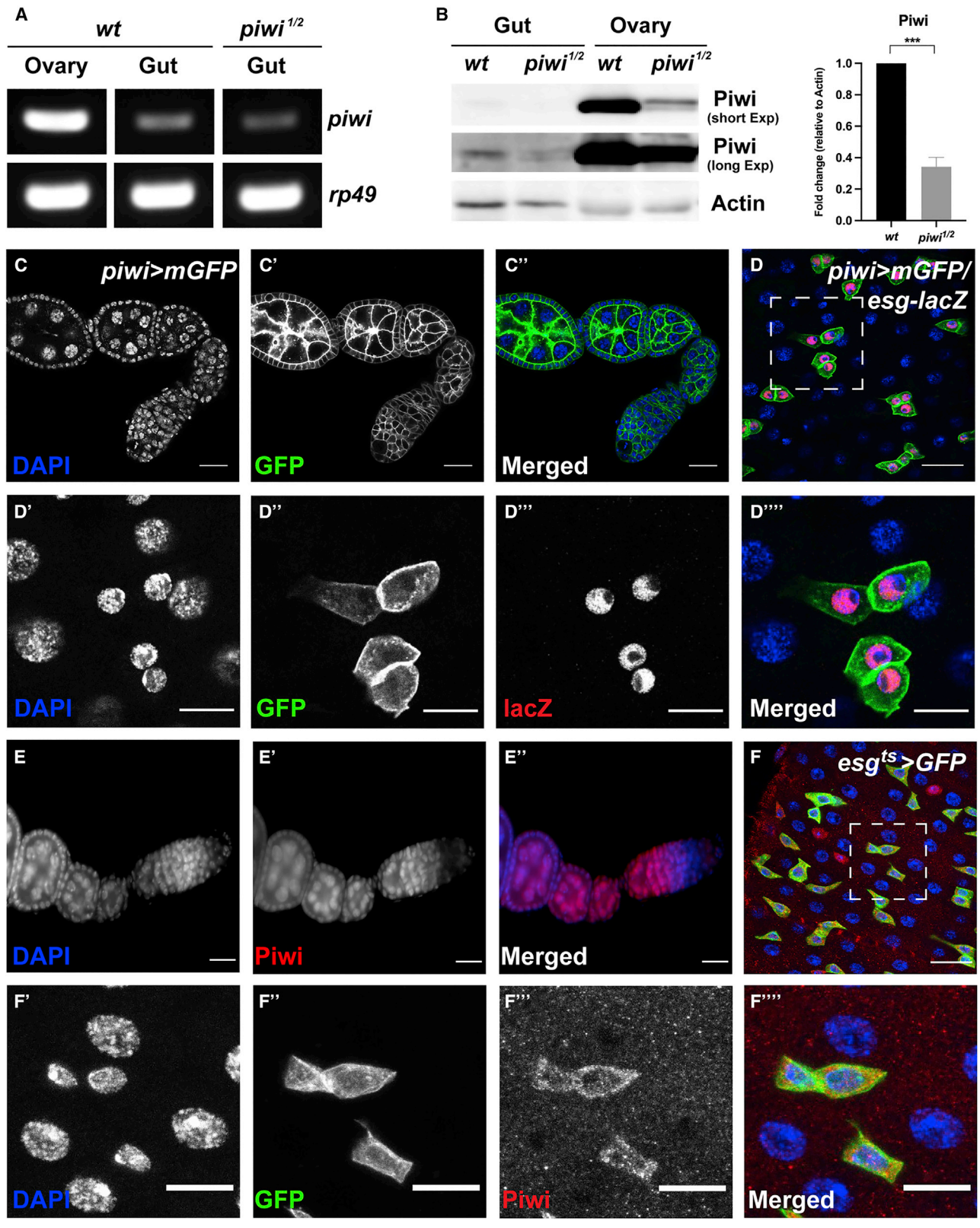

(legend on next page)

In addition to TE silencing, Piwi plays an essential role in regulating *Drosophila* germline stem cell maintenance; however, its roles in somatic tissues remain largely unexplored. Only a few studies have implicated the somatic function of Piwi outside the gonad. For instance, Piwi co-localizes with Heterochromatin Protein 1a (HP1a) on polytene chromosomes and may be involved in heterochromatic gene silencing in the larval salivary gland (Brower-Toland et al., 2007). In addition, *piwi* acts as a strong epigenetic suppressor of positional effect variegation in the adult eye (Yin and Lin, 2007; Pal-Bhadra et al., 2004; Gu and Elgin, 2013). The expression of Piwi has also been reported in the adult fat body to modulate lipid droplet synthesis and storage (Jones et al., 2016). More recently, Piwi was reported to be critical for heterochromatin maintenance, retrotransposon silencing, DNA integrity, and the long-term upkeep of ISCs under regenerative conditions induced by damaging insults or proliferative pressure (Sousa-Victor et al., 2017). However, this somatic function of Piwi could be induced by stress, just like the ectopic expression of PIWI proteins in somatic tissues when they become cancerous (Ross et al., 2014). Therefore, the function of Piwi in the gut under normal physiological conditions remains unknown.

In this study, we investigated the function of Piwi in regulating intestinal homeostasis and function under normal physiological conditions. We show that depleting Piwi in the gut decreased the number of ISCs during gut development, reduced EB maintenance, and induced cell death in differentiated ECs, compromising the gut epithelium. In addition, we found that *piwi* is required to silence several TEs in the gut, whereas *aub* or *ago3* are only required for silencing a few TEs. Moreover, we show that the epithelial functions of *piwi* in the intestine, possibly including the TE silencing function, play a significant role in sustaining the normal lifespan of the adult flies. Finally, our mRNA sequencing analysis revealed that many genes involved in metabolism and oxidation-reduction are differentially expressed in the adult *piwi* mutant gut, implying that intestinal Piwi achieves its function mainly by regulating these genes to maintain homeostasis.

RESULTS

Piwi is expressed in intestinal stem cells and enteroblasts

We first analyzed *piwi* mRNA expression in the adult gut by RT-PCR. *Piwi* mRNA was expressed at a very low but clearly detectable level in the wild-type adult gut, in contrast to its strong expression in the adult ovary (Figure 1A). The mRNA level was reduced in transheterozygous $piwi^{1/2}$ mutant guts and hypomorphic $piw^{2/2}$ mutant ovaries (Figures 1A and S1A), indicating the specificity of the RT-PCR. To examine Piwi protein expression, we performed western blotting using a commercial anti-Piwi antibody (sc-390946) (Jones et al., 2016; Sousa-Victor et al., 2017). However, we found that this antibody does not show clear specificity in the ovary (Figures S1B and S1C).Therefore, we decided to use another antibody, 4K5, (Gonzalez et al., 2021) to detect Piwi expression. This antibody specifically recognized a Piwi-sized protein that was highly expressed in the wild-type ovary but was drastically reduced in the ovaries of $piwi^{1/2}$ and two Piwi protein null mutants, *piwi>gal4* (Stein et al., 2019) and $piwi^{g1}$ (Senti et al., 2015), confirming its specificity (Figures 1B and S1C). Using 4K5, we observed a weak Piwi band in the wild-type gut that was significantly reduced in the $piwi^{1/2}$ mutant gut (Figure 1B), indicating that the Piwi protein is expressed in the adult gut at a low level.

To further characterize the expression pattern of Piwi in the gut, we combined the *piwi-gal4* line with a *UAS*-membrane-bound *GFP* (*mGFP*) line, allowing *piwi-gal4*-driven mGFP expression *in vivo*. This *piwi* reporter line exhibited a high level of *piwi* expression in the adult ovary (Figures 1C–1C″), recapitulating the endogenous Piwi expression pattern and validating the faithfulness of this line in reporting *piwi* expression. We then examined this reporter expression in the gut and found that mGFP is specifically expressed in small diploid cells but not in large polyploid enterocytes (Figure 1D). Strikingly, these GFP-positive cells coincide with *esg-lacZ*-positive cells, which label ISCs and EBs (Figures 1D′–1D′′′′), indicating that *piwi* is specifically expressed in these cells. In addition, strong mGFP expression was detected in larval testes,

Figure 1. Piwi is expressed in ISCs and EBs

(A) RT-PCR data of *piwi* mRNA expression in w^{1118} and $piwi^{1/2}$ guts.

(B) Western blotting image (left) and its quantification (right) of Piwi protein expression in the adult w^{1118} and $piwi^{1/2}$ gut. Exp: exposure. n = 3.

(C and D′′′′) The expression pattern of *piwi-gal4*-driven mGFP in the ovary (C-C″) and female adult gut (D-D′′′′). The *esg-lacZ* labels ISCs and EBs. (D′-D′′′′) are magnified images of the dot-lined box in (D).

(E and F′′′′) Anti-Piwi antibody (4K5) staining in the ovary (E-E″) and *esg-gal4; tub-gal80^{ts}, UAS-GFP* female gut (F). (F′-F′′′′) are magnified images from the dot lined box region in (F). DAPI indicates DNA. Scale bars, 20 μm in (C)–(F), 10 μm in (D′–D′′′′) and (F′–F′′′′). Statistical analysis: unpaired t test, ***p < 0.001.

See also Figures S1 and S2.

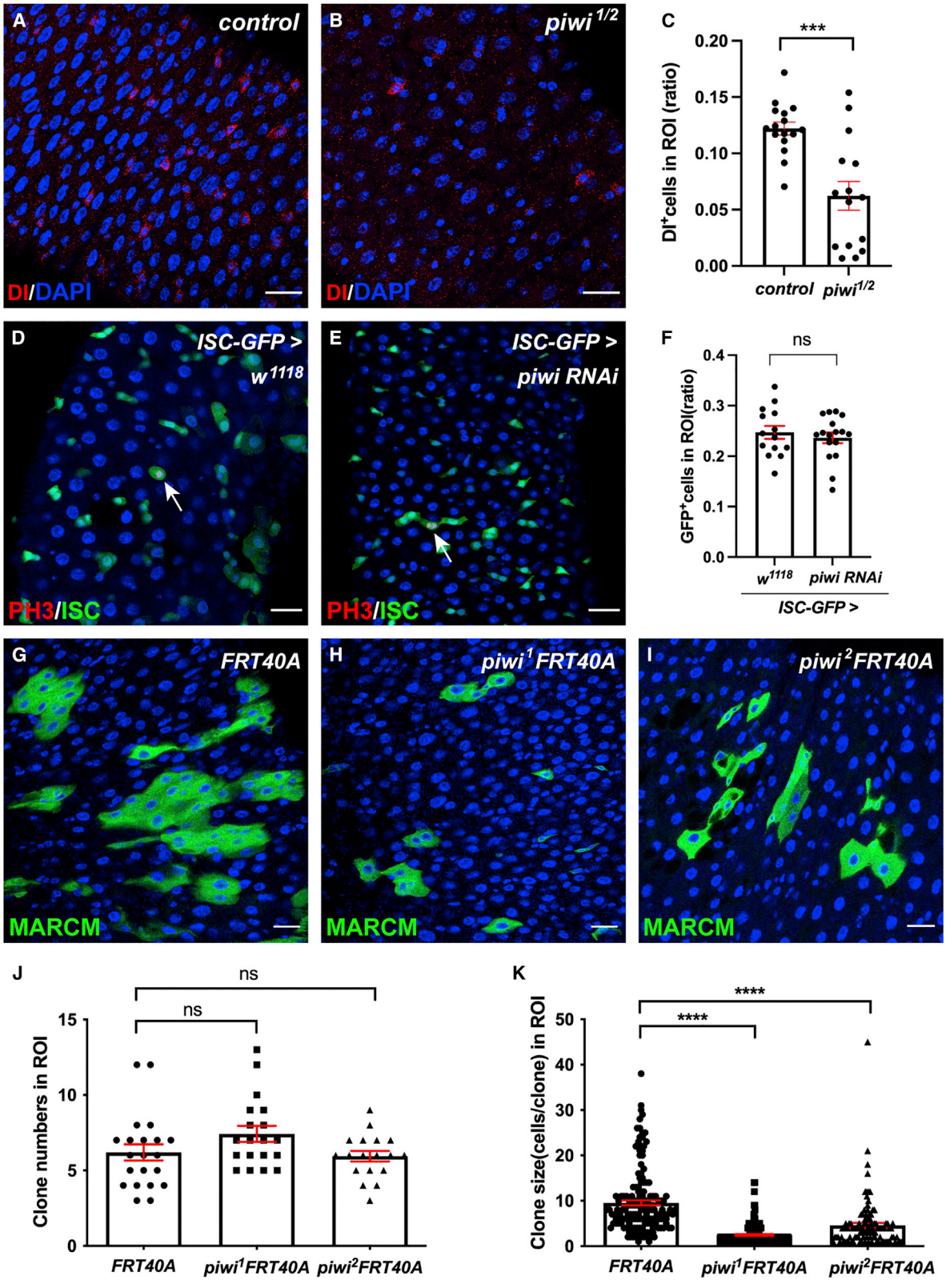

(legend on next page)

salivary glands, and adult midgut precursor islets (Figure S2), confirming *piwi* transcription in these organs and cells. Immunostaining using 4K5 was then conducted to further decipher Piwi expression pattern in the gut. As expected, Piwi was expressed in the adult ovary (Figures 1E–1E″) and gut, where it co-localizes with *esg-gal4 driven* GFP-positive ISCs and EBs but not differentiated cells (Figures 1F–1F‴). In addition, Piwi are mostly in the cytoplasm, indicating a likely post-transcriptional function. Together, these data confirmed that Piwi is specifically expressed in the intestinal stem cell and progenitor cells.

Piwi deficiency compromises the establishment of the ISC population during gut development

To assess if Piwi regulates ISCs and their lineage, we first examined if loss of Piwi affect ISC numbers by using the anti-Delta (DI) antibody to mark ISCs. The number of ISCs is significantly reduced in the $piwi^{1/2}$ mutant gut as compared with the wild-type control (Figures 2A–2C). To further delineate whether the reduced number of ISCs is due to a defect in establishing the ISC population during gut development and/or the post-developmental maintenance of ISCs in the adult gut, we crossed a *UAS-GFP* reporter line driven by the ISC-specific *esg-gal4* into *tub-gal80^{ts} and Su(H)-gal80* background to generate the *esg-gal4 tub-gal80^{ts} UAS-GFP/+; Su[H]-gal80/+* flies (hereafter referred to as *ISC-GFP).* In these flies, the *esg-gal4*-driven expression of *UASp-GFP* was inhibited in both ISCs and EBs by *tub-gal80^{ts}* under the permissive temperature (22–25°C). However, under the restrictive temperature (29–30°C), the *esg-gal4:UAS-GFP* became expressed in ISCs, but was still inhibited in EBs by the EB-specific Gal4 suppressor *Su(H)-gal80*, resulting in ISC-specific expression of GFP. When the *UAS-piwi* RNAi line was further introduced into the *ISC-GFP* flies (the resulting flies are hereafter referred to as *ISC-GFP > piwi RNAi),* the Gal80-Gal4 system drove the UAS-*piwi* RNAi expression to knock down *piwi* mRNA specifically in adult ISCs. This knockdown did not change the number of ISCs when compared with the wild-type control (Figures 2D–2F), indicating that Piwi has no obvious function in maintaining ISCs in the adult gut. Therefore, the decreased number of ISCs in the $piwi^{1/2}$ mutant gut is likely due to defects in establishing the ISC population during pre-adult development.

Piwi is required for EB maintenance

We then performed the "mosaic analysis of a repressible cell mark" (MARCM) to track ISC proliferation, differentiation, and death in a *piwi*/+ background (Lee and Luo, 2001). As shown in Figures 2G–2I and 2J, the total numbers of induced clones in $piwi^{1/+}$ and $piwi^{2/+}$ guts were comparable to those of wild-type clones in similar gut regions, further confirming that $piwi^{1/+}$ and $piwi^{2/+}$ guts had a normal number of ISCs. However, homozygous $piwi^{1}$ and $piwi^{2}$ mutant clones were significantly smaller due to reduced number of cells in these clones (Figures 2G–2I and 2K), indicating that the loss of Piwi may decrease the mitotic ability of ISCs or increase apoptosis, or both.

To distinguish between these two possibilities, we measured the mitotic index of ISCs in *piwi* mutant guts by using anti-phosphorylated histone 3 (PH3) antibody to specifically label mitotic chromosomes. The number of dividing ISCs was comparable in the wild-type and two different *piwi* mutant guts (Figures 3A–3D). To confirm these results, we specifically downregulated Piwi expression in the adult gut for 7 days either in ISCs (Figures 2D and 2E) or EBs (Figures 3E and 3F), labeled ISCs with *ISC-GFP* and EBs with *Su(H)GBE-Gal4/+;UAS-GFP tub-gal80^{ts}/+* (referred to as *Su(H)GBE^{ts}-gal4*) (Wang et al., 2014), and then measured the mitotic activity in the gut. Either ISC- (Figure 3I) or EB-specific (Figure 3J) *piwi* knockdown did not affect the number of PH3-positive cells, confirming that depleting Piwi does not affect ISC division in the gut.

We then performed the TUNEL assay to examine cell death. We detected more TUNEL-positive cells in the $piwi^{1/2}$ mutant gut (Figures 3H and 3L) than in the wild-type gut (Figures 3G and 3L). Notably, TUNEL signals appeared to be more enriched in the large polyploid cells than small diploid cells in the $piwi^{1/2}$ mutant gut, indicating that the loss of Piwi induced the death of more ECs than ISC and EBs. Since ISC numbers were not changed upon Piwi depletion in this stage as shown in Figure 2F, we sought to examine if loss of Piwi could change EB numbers. As shown

Figure 2. Piwi deficiency compromises the establishment of the ISC population during gut development

(A and B) Anti-Dl antibody staining in 5-day-old wild-type (A) and $piwi^{1/2}$ (B) posterior midguts.

(C) The number of DI-positive ISCs in the region of interest (ROI) in the wild-type (n = 16) and $piwi^{1/2}$(n = 15) gut.

(D and E) Anti-PH3 antibody staining in control (D) and upon *piwi* knockdown in ISCs (E) driven by the ISC-GFP system for 7 days. White arrows indicate PH3-positive ISCs.

(F) Quantification of GFP-positive ISCs in the ROI from control (n = 14) and *piwi* knockdown (n = 17) guts.

(G–I) MARCM analysis in the wild-type (G), $piwi^{1}$(H), and $piwi^{2}$(I) guts.

(J) The number of induced MARCM clones in the ROI in the wild-type (n = 21), $piwi^{1}$ (n = 19), and $piwi^{2}$ (n = 18) posterior midgut.

(K) The number of cells in each clone from wild-type (n = 158), $piwi^{1}$ (n = 159), and $piwi^{2}$ (n = 107) mutant guts. ROI is approximately in the R4/R5 region (Buchon et al., 2013). Statistical analysis: unpaired t test, ***p < 0.001, ****p < 0.0001. ns, no significance. Error bars represent SEM. Scale bars, 20 μm.

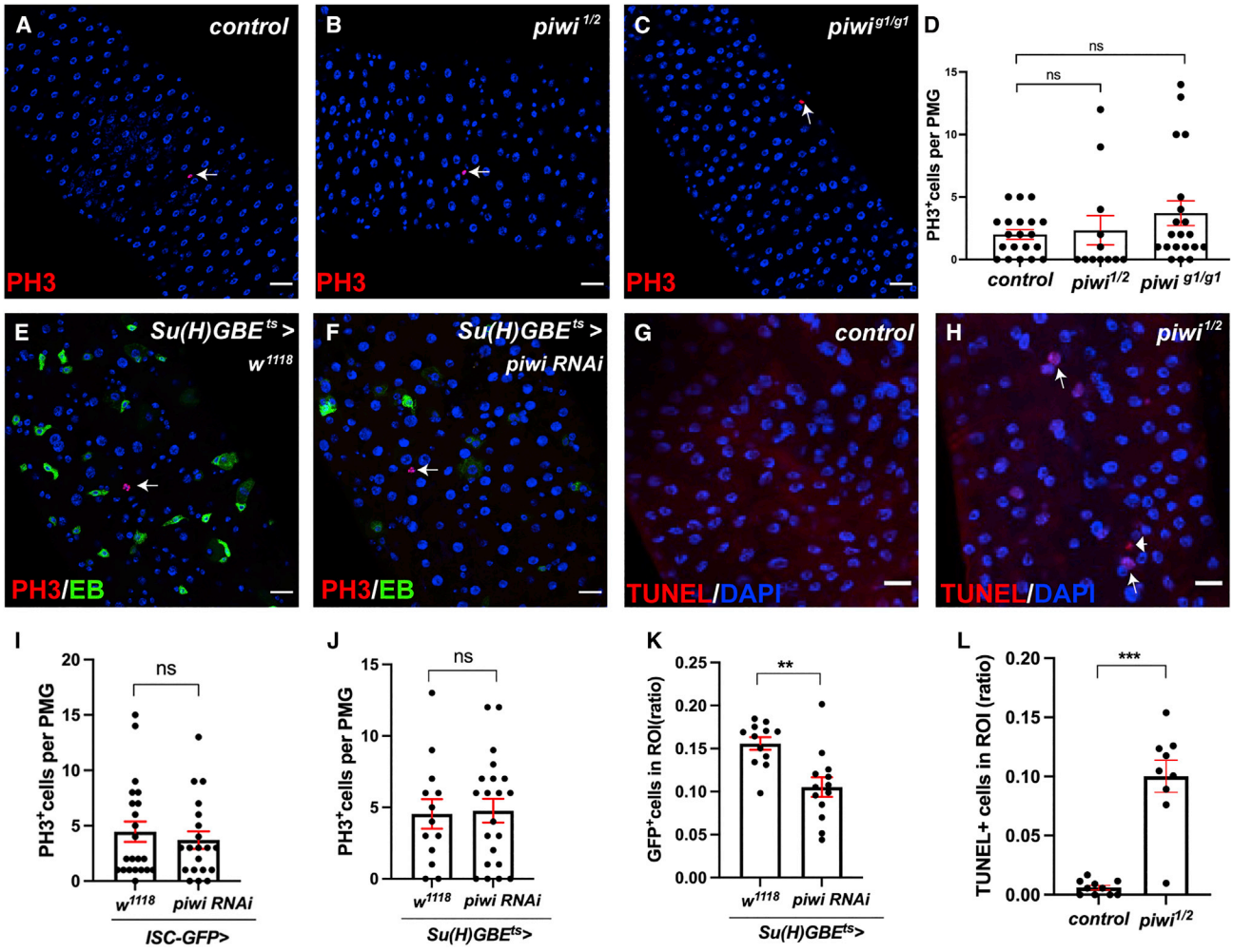

Figure 3. Piwi is required for EB maintenance

(A–C) Anti-PH3 antibody staining in the 5-day-old wild-type (A), *piwi*$^{1/2}$ (B), and *piwi*$^{g1/g1}$(C) posterior midgut.

(D) Quantification of the number of PH3-positive cells in the wild-type (n = 20), *piwi*$^{1/2}$ (n = 12), and *piwi*$^{g1/g1}$(n = 20) posterior midgut (PMG).

(E and F) Anti-PH3 antibody staining in control (E) and upon *piwi*-knockdown in EBs driven by *Su(H)GBE*^{ts}*-gal4* for 7 days (F). White arrows indicate PH3-positive dividing ISCs.

(G and H) Representative images of the TUNEL assay in wild-type control (G) and *piwi*$^{1/2}$ (H) guts. White arrows and arrowhead indicate TUNEL-positive cells in large polypoid and small diploid cells, respectively.

(I and J) Quantification of the number of PH3-positive cells in the PMG from control (n = 22) and upon *piwi* downregulation (n = 20) in ISCs (I) and from control (n = 12) and *piwi* downregulation (n = 13) in EBs (J).

(K) Quantification of the number of GFP-positive EBs in the ROI from control (n = 13) and upon *piwi* downregulation (n = 21) in EBs.

(L) Quantification of TUNEL-positive cells in the wild-type control (n = 10) and *piwi*$^{1/2}$ (n = 9) gut. ROI, region of interest (approximately in the R4/R5 region). Statistical analysis: unpaired t test, **p < 0.01, ***p < 0.001, ns, no significance. Error bars represent SEM. Scale bars, 20 μm. See also Figure S3.

in Figures 3E, 3F, 3K, and S3H, EB-specific knockdown of Piwi for 7 days reduced EB number in the gut, indicating that Piwi is cell-autonomously required for EB maintenance.

Piwi is not required for ISC differentiation to EEs

We then examined ISC differentiation to EEs in the *piwi*$^{1/2}$ mutant gut by staining for anti-Prospero, a Pan-endocrine EE cell marker. The ratio of EE cells was not changed in the *piwi*$^{1/2}$ mutant gut (Figures S3A, S3B′, and S3E), indicating that loss of Piwi has no obvious effect on ISC-to-EE differentiation. To more closely examine the function of Piwi during ISC-to-EE differentiation, we combined a *piwi* RNAi line with the *esg-gal4*^{ts} *flip-out (F/O)* system (Jiang et al., 2009) to track Piwi effect on EE differentiation. In

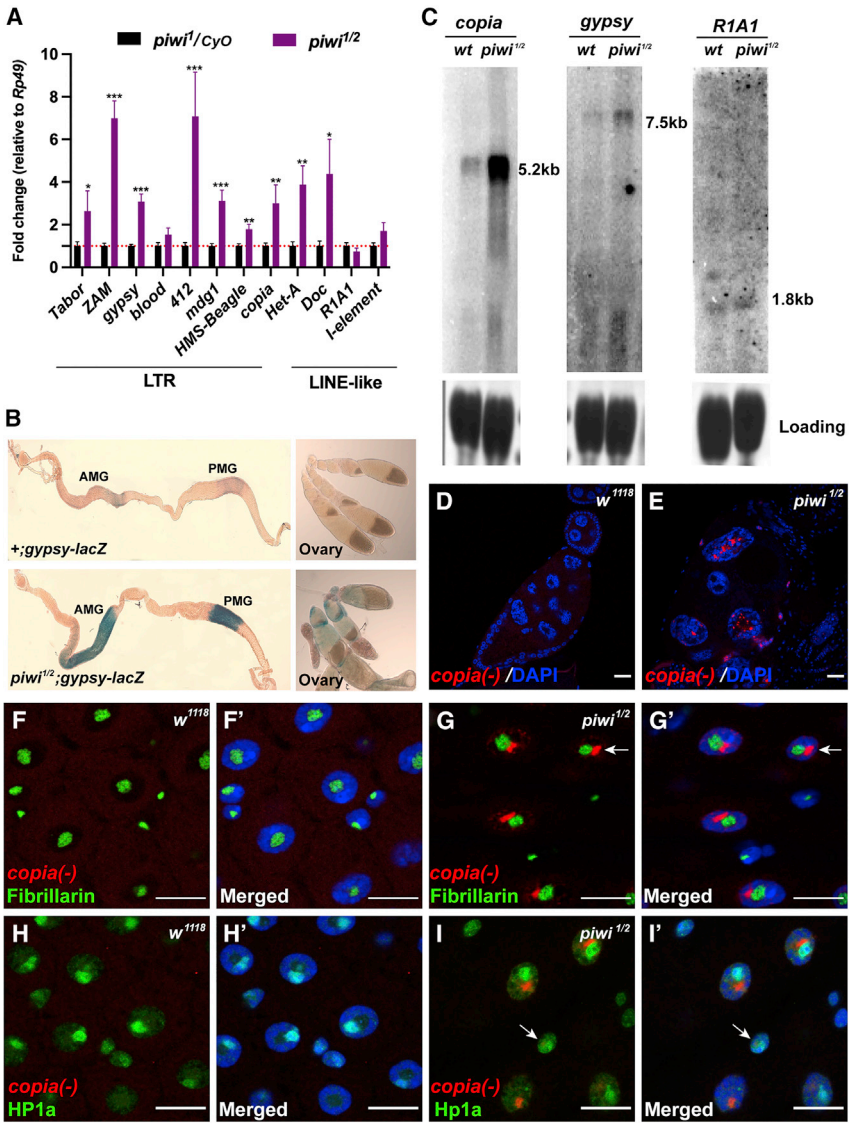

Figure 4. Zygotic Piwi suppresses retrotransposon expression in the gut

(A) RT-qPCR data of TE expression in 5-day-old *piwi*^{1}*/CyO* (black) and *piwi*$^{1/2}$ (purple) guts. n = 9. Statistical analysis: multiple unpaired t test, *p < 0.05, **p < 0.01, ***p < 0.001. Error bars represent SEM.

(B) β-galactosidase staining in the 5-day-old *gypsy-lacZ*-containing wild-type (n = 14) and *piwi*$^{1/2}$ (n = 23) guts (left) and ovaries (right). AMG, anterior midgut; PMG, posterior midgut.

(C) Northern blot images of *copia*, *gypsy*, and *R1A1* expression in the wild-type and *piwi*$^{1/2}$ gut. Methylene blue staining indicates the equal loading of total RNA.

(D and E) Representative images of FISH using the *copia* antisense (−) probe in wild-type (D) and *piwi*$^{1/2}$ ovaries (E).

(F–I′) Representative images of the *copia* FISH and co-immunostaining with anti-Fibrillarin (F-G′) or anti-Hp1a (H-I′) antibodies in the wild-type (F-F′, H-H′) and *piwi*$^{1/2}$ (G-G′, I-I′) guts. DAPI indicates DNA. White arrows: *copia* RNA-positive EBs. Scale bars,10 μm. See also Figures S4 and S5.

the wild-type gut, *esg-gal4*^{ts}-driven GFP expression in ISCs and EBs upon shifting temperature from 22–24°C–29°C produced a cluster of daughter cells that were labeled by *act-gal4*-driven GFP (Figures S3C–S3C‴). The depletion of *piwi* led to the formation of smaller GFP clusters (Figures S3D–S3D‴ and S3F), confirming the results from MARCM analysis. However, the ratio of EE cells within each examined GFP cluster was not changed in the *piwi*-downregulated clusters (Figure S3G), suggesting that Piwi is not required for ISC-to-EE differentiation.

Zygotic Piwi suppresses retrotransposon expression in the gut

Piwi is well known to suppress TE expression in the germline to maintain genome integrity. To examine whether Piwi has a similar effect in the gut, we measured the expression of representative retrotransposons in the *piwi*$^{1/2}$ mutant gut by RT-qPCR. Nine out of 12 examined TEs, including seven long terminal repeat type TEs and two long interspersed nuclear element (LINE)-like type TEs, were significantly upregulated in the *piwi*$^{1/2}$ mutant gut as compared with the *piwi*^{1}*/CyO* heterozygous control (Figure 4A). These TEs were also drastically upregulated in the *piwi*$^{1/2}$ mutant gut when compared with the wild-type control (Figures S4A and S4B). In addition, *piwi-gal4* and *piwi*^{s1} mutant guts also exhibited elevated expression of some TEs (Figure S4C), indicating that Piwi represses TE expression in the gut.

To validate TE activation in the *piwi*$^{1/2}$ mutant gut, we further examined *gypsy* and *copia* expression in the

piwi$^{1/2}$ mutant gut by using a reporter assay and northern blotting analysis. The *gypsy-lacZ* reporter line showed much higher expression in both the anterior and posterior part of the *piwi*$^{1/2}$ mutant midgut than that in the wild-type gut (Figure 4B), indicating that Piwi represses *gypsy* transcription in these two midgut regions. Furthermore, our northern blotting data confirmed that the RNA levels of both *copia* and *gypsy*, but not *R1A1* and *I-element*, are drastically upregulated in the *piwi*$^{1/2}$ mutant gut (Figures 4C and S4B). Taken together, these data support that Piwi silences a subset of TEs in the adult gut.

Recent studies show that maternal Piwi is capable of suppressing TE expression in adult tissues by perturbation of heterochromatin formation presumably in early embryonic stages (Akkouche et al., 2017; Gu and Elgin, 2013). To examine whether maternal Piwi has any effect on TE expression in the adult gut, we depleted maternal Piwi expression by crossing the maternal *actin (MAT)-gal4* driver with two different *piwi* RNAi lines (Gonzalez et al., 2021). In these crosses, progeny from F0 females with the *MAT-gal4>piwi* RNAi were largely devoid of maternal Piwi expression, while those from F0 females with the *MAT-gal4>GFP* RNAi retained both maternal and zygotic Piwi expression (Gonzalez et al., 2021). We measured TE expression in F1 adult female guts. Five of the six examined TEs were not upregulated in the maternally Piwi-depleted guts, except for *gypsy* RNA that appeared to be upregulated but the upregulation is non-significant, with its level much lower than that of the *piwi*$^{1/2}$ mutant gut (compare Figures S4D and 4A). These results indicate that maternal Piwi does not play an obvious role in suppressing TEs in the adult gut. Thus, TE de-silencing in the *piwi* mutant gut is mainly, if not exclusively, caused by loss of zygotic Piwi expression.

Furthermore, we investigated in which gut cell type TEs are activated in the *piwi* mutant. Fluorescence *in situ* hybridization (FISH) was performed to examine the expression pattern of *copia*, one of the most activated TEs in the *piwi*$^{1/2}$ mutant gut. The antisense *copia* probe (Figures 4D, 4E, and S5E), but not the sense *copia* probe (Figures S5A–S5D), manifested strong nuclear signal in the *piwi*$^{1/2}$ or *piwi*$^{2/2}$ mutant ovaries, indicating the specificity of our FISH. Strikingly, *copia* RNA is mostly accumulated in large polyploid differentiated ECs and showed very weak to no expression in small diploid cells in *piwi*$^{1/2}$ (Figures 4G–4G′ and 4I–4I′) and *piwi*$^{2/2}$ (Figures S5F–S5F″) mutant guts, while the wild-type control showed no *copia* signal (Figures 4F–4F′ and 4H–4H′). To further determine the subcellular localization of activated *copia* RNA in these differentiated ECs, we combined FISH with immunostaining to label the dense fibrillar component of the nucleolus using anti-Fibrillarin antibody and the heterochromatin compartment using anti-HP1a antibody. In the *piwi* mutant gut, *copia* RNA appears to be mostly enriched adjacent to the nucleolus (Figures 4G–4G′), but is not present in the heterochromatin compartment in the nucleus of the ECs (Figures 4I–4I′). These data indicate that *copia* activation in the *piwi* mutants mostly occurs in the differentiated ECs. Interestingly, co-immunostaining with LacZ and DI in the gut showed that the *gypsy-lacZ* is likely activated in *piwi*-deficient stem cells, but not in differentiated cell types (Figures S5G–S5H‴), implying that *copia* and *gypsy* RNA are activated in different cell types in the *piwi* mutant gut.

Piwi in ISCs and EBs is capable of suppressing TE expression in the gut

To resolve the paradoxical findings that Piwi is specifically expressed in ISCs and EBs yet *copia* de-silencing was observed in ECs, we downregulated Piwi expression in ISCs and EBs and measured TE expression. As shown in Figures S4E and S4F, four out of nine examined retrotransposons (*mdg1*, *copia*, *Het-A*, *Doc*) were significantly upregulated, but the expression of the other five retrotransposons (*Tabor*, *blood*, *412*, *Rt1a*, *I-element*) was not changed. These data suggested that Piwi expression in the ISCs and EBs can prevent the expression of these four TEs in ECs and that the activation of other five TEs may require greater extents of Piwi reduction.

Aub and Ago3 have minor effect on TE silencing and the siRNA pathway contributes to TE silencing in the gut

To explore if the other two PIWI subfamily proteins, Aub and Ago3, have similar effects on TE silencing in the gut, we examined their expression by using RT-PCR. Both *aub* and *ago3* were expressed in the wild-type gut, albeit at lower levels than in the ovary (Figure 5A). Their expression was drastically decreased in the *aub* $^{HN22/QC42}$ and *ago3* $^{T2/T3}$ (Li et al., 2009) transheterozygous mutant guts, respectively. However, western blotting and immunostaining did not detect Aub or Ago3 protein in the adult gut, even though under the same condition both Aub and Ago3 showed high levels of expression and expected cytoplasmic localization in the ovary (Figures 5B–5C″ and S6). This indicates that Aub and Ago3 are present in the gut at extremely low levels. Furthermore, RT-qPCR analysis showed that *ZAM, copia*, and *Het-A* were significantly upregulated both in *aub* and *ago3* mutant guts but *Tabor* was only selectively upregulated in the *aub* mutant gut (Figure 5D). Other examined retrotransposons were not significantly activated by the loss of either Aub or Ago3. These data indicate that Aub and Ago3 are capable of selectively silencing some

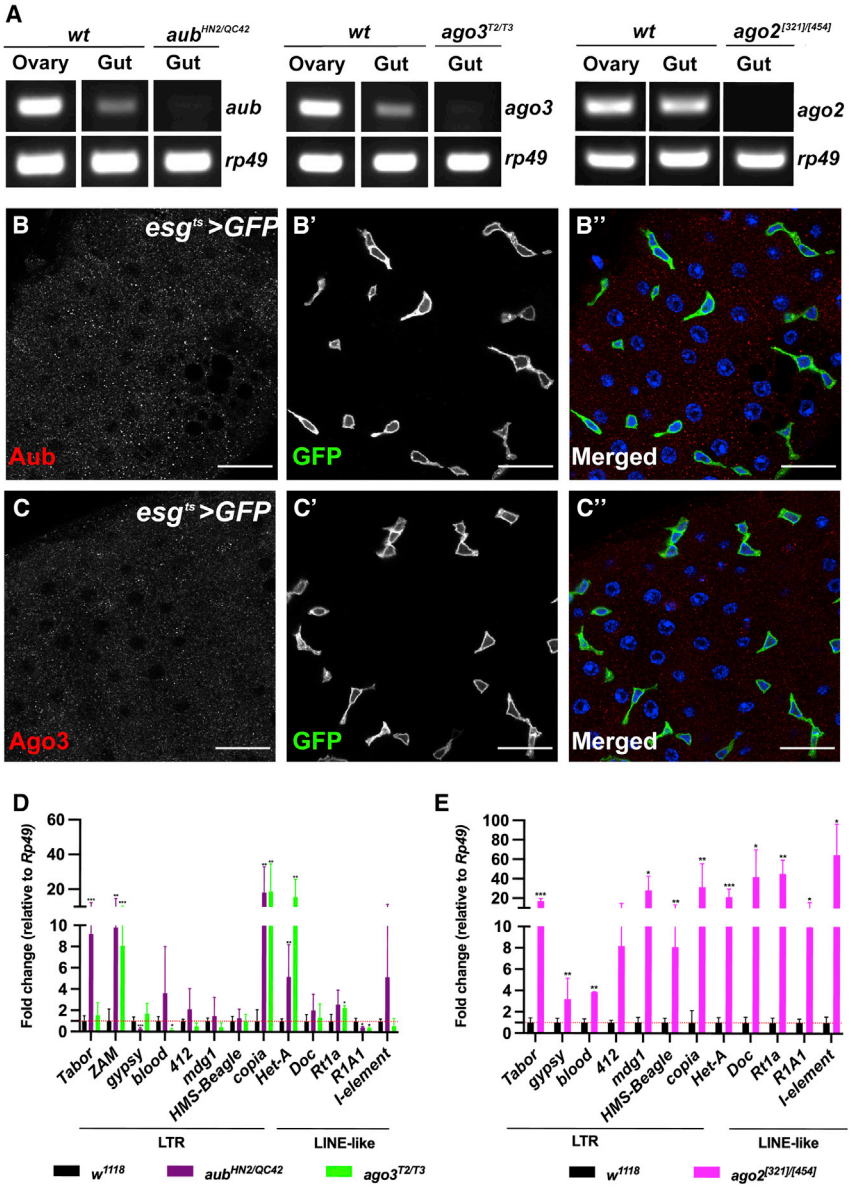

Figure 5. Aub and Ago3 have minor effect on TE silencing and the siRNA pathway contributes to TE silencing in the gut

(A) RT-PCR data of *aub* (left), *ago3* (right), and *ago2* (right) mRNA expression in the adult control and $aub^{HN2/QC42}$, $ago3^{T2/T3}$, and $ago2^{321/454}$ guts, respectively. n = 3–4.

(B and C″) Anti-Aub (B-B″) or anti-Ago3 (C-C″) immunostaining in the adult gut ISC/EB-reporter line (esg^{ts} > GFP). Scale bar, 20 μm.

(D and E) RT-qPCR data of TE expression in 5-day-old adult wild-type (black) and $aub^{HN2/QC42}$(purple), $ago3^{T2/T3}$ (green), and $ago2^{321/454}$ (magenta) mutant guts, respectively. n = 3. Statistical analysis: multiple unpaired t test, *p < 0.05, **p < 0.01, ***p < 0.001. Error bars represent SEM.

See also Figures S6 and S7.

TEs in the gut, probably indirectly. However, their TE-silencing effect in the gut is not as strong as that of Piwi.

In addition, we also found that Ago2, an Argonaute subfamily protein, is expressed in the gut and represses a variety of TE expression (Figures 5A and 5E), suggesting that Ago2 also silences TE expression in the adult gut. Since Ago2 has been reported to repress TE expression in the *Drosophila* adult head (Kawamura et al., 2008; Ghildiyal et al., 2008; Czech et al., 2008; Chung et al., 2008), we analyzed TE expression in these *ago* mutant heads, respectively. Loss of *ago2* de-silenced many retrotransposons in the adult head (Figures S7A and S7C), while loss of Piwi or Ago3 only selectively derepressed some retrotransposons (Figures S7A and S7B), indicating that the Ago2 acts as a major TE repressor in the head.

Intestinal *piwi* regulates the expression of hundreds of genes in the gut and contributes to adult survival

To investigate how Piwi regulates the global mRNA gene expression, we performed mRNA-seq in the wild-type and $piwi^{1/2}$ mutant guts. We identified 899 differentially expressed genes (DEGs), with 444 downregulated (Table S1) and 455 upregulated genes (Table S2) in the $piwi^{1/2}$ mutant gut (Figure 6A). Gene Ontology analyses according to "Biological process" of significantly downregulated genes revealed enrichment of genes in glutathione metabolic

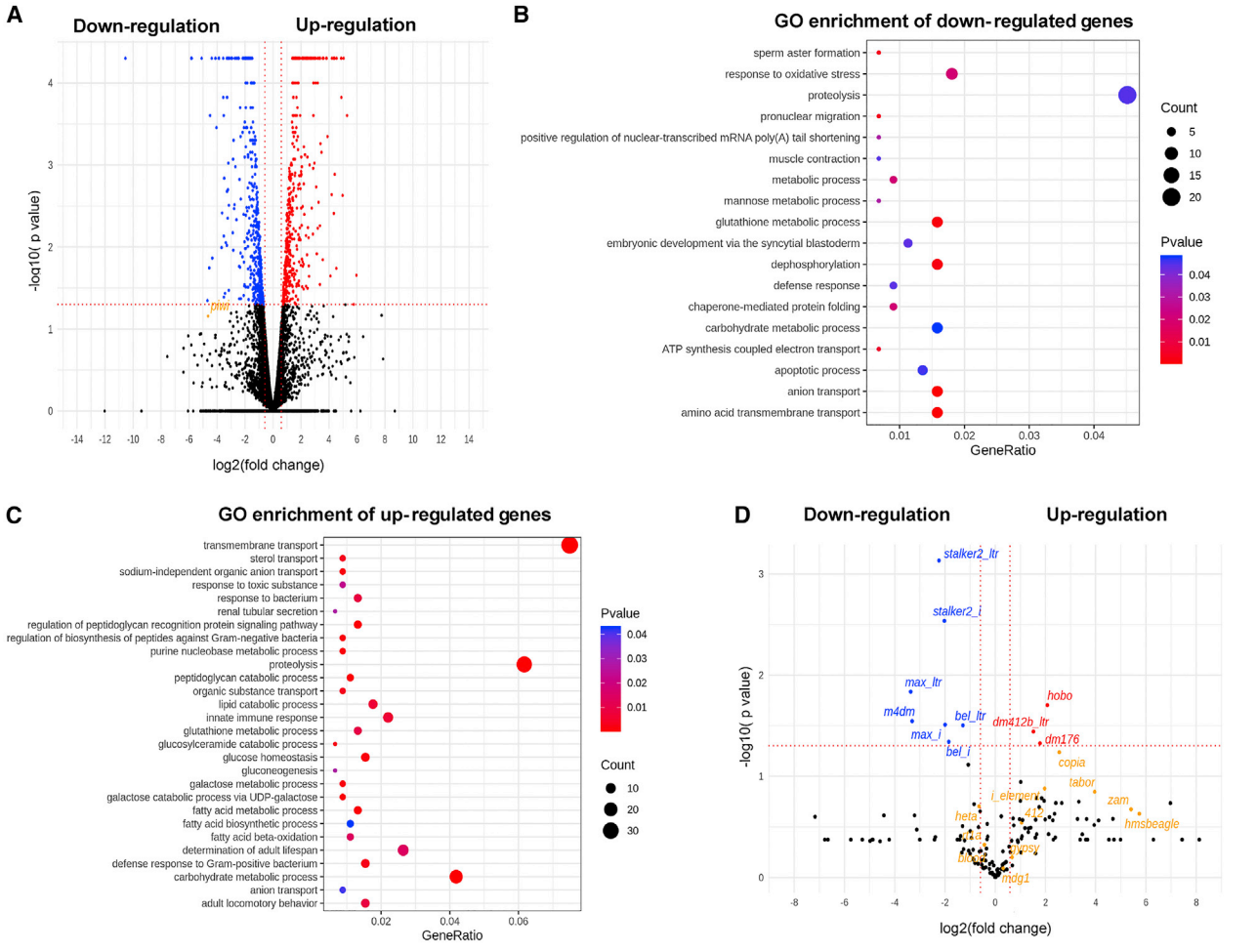

(legend on next page)

process, response to oxidative stress, amino acid transmembrane transport, and proteolysis in the *piwi*$^{1/2}$ mutant gut (Figure 6B). The upregulated genes are enriched in transmembrane transport, carbohydrate and glutathione metabolism, and proteolysis (Figure 6C). These analyses indicate that Piwi is involved in regulating broad metabolic and transport processes in the gut epithelium to achieve gut homeostasis.

In addition to protein-coding genes, we found that 53 TEs are upregulated by ≥2-fold in the *piwi*$^{1/2}$ mutant gut, among which 50 were shown to be upregulated in the *piwi* mutant ovary (see supplemental experimental procedures). In addition, 33 transposons are downregulated by ≥ 2-fold in the *piwi*$^{1/2}$ mutant gut (Table S3). The trend of TE activation was confirmed by RT-qPCR and Northern results, even though most of them did not show statistically significant p value ($p \leq 0.05$; Figure 6D). This indicates that Piwi prevents TE expression in the gut.

To detect possible existence of piRNA in the gut, we performed small RNA-seq to profile the distribution of 16 nt to 36 nt RNAs in the adult gut. Surprisingly, small RNAs of ~18 to 21 nt were more abundant in the *piwi*$^{1/2}$ mutant gut than in the wild-type gut (Figure 6E). In addition, there were ~23 to 29 nt small RNAs present in *piwi*$^{1/2}$ mutant samples. Moreover, many small RNA species were more abundant in the *piwi*$^{1/2}$ mutant gut than in the wild-type gut (Figure 6E). Thus, the biogenesis of these small RNAs is somehow repressed by Piwi. Therefore, these small RNAs are unlikely piRNAs. To further examine whether these small RNAs (20 nt to 32 nt) are piRNAs, we analyzed their base composition, which does not show canonical piRNA signatures such as the first U bias or the 10th A enrichment (Figures 6F and 6G). Therefore, these analyses confirm that canonical piRNAs are not detected in the adult gut and that Piwi-mediated TE silencing in the gut may be piRNA-independent.

Interestingly, we also identified 43 small RNAs of 20 to 32 nt that are downregulated in the *piwi* mutant gut (Table S5), indicating that Piwi is required directly or indirectly for the expression of these small RNAs in the gut. These small RNAs map to protein-coding genes (63%), transposons (28%), ncRNA-coding sequences (7%), and other repeats (2%). Whether they are piRNAs awaits further investigation.

Finally, we assessed the biological function of the Piwi-mediated gene regulation in the adult gut. First, we performed survival assay to examine the effect of Piwi on adult lifespan. Interestingly, all three different *piwi* mutant females exhibited shorter lifespan when compared with the control (Figure 7A). In order to specify the role of intestinal Piwi in regulating lifespan, we downregulated Piwi expression specifically in ISCs and EBs in the adult stage using two different *piwi* RNAi lines separately, followed by measuring adult longevity. Flies with Piwi-deficient ISCs and EBs showed a similarly shortened adult lifespan (Figure 7B), implying that Piwi expression in ISCs and EBs is the main contributing factor to adult survival. In addition, loss of Aub, Ago3, or Ago2 also affects adult lifespan, indicating that other Ago proteins also contribute to adult survival (Figures 7C and 7D).

DISCUSSION

Piwi has been extensively studied in the germline due to its strong expression and clear phenotype in fertility and transposon silencing in germ cells. However, Piwi function in somatic tissue is largely unknown. Here, we reported Piwi function in the *Drosophila* adult gut epithelium. We found that Piwi is expressed in ISCs and EBs under homeostatic conditions, albeit at a low level, and that the loss of Piwi affects ISC establishment, compromises EB maintenance, and induces cell death mostly in ECs (Figures 7E and 7F). Specifically, we showed that Piwi expression in ISCs during pre-adult development

Figure 6. Intestinal Piwi regulates hundreds of genes

(A)Volcano plot of DEGs in the *piwi*$^{1/2}$ gut as compared with the wild-type gut. Upregulated, downregulated, and insignificantly changed genes are highlighted in red, blue, and black dots, respectively. The orange dot indicates *piwi*. The horizontal dashed red line indicates p value = 0.05 and two vertical dashed red lines indicate fold change = 1.5.

(B and C) Gene ontology analyses of significantly down- (B) and upregulated (C) DEGs in the *piwi*$^{1/2}$ gut.

(D) Volcano plot of TE expression change in the *piwi*$^{1/2}$ gut as compared with the wild-type gut. Upregulated, downregulated, and insignificantly changed genes are colored in red, blue, and black dots, respectively; 0.001 was added to expression level for logarithm calculation on fold change. Orange dots highlight experimental verified TEs shown in Figure 4A.

(E) Size profile of small RNAs (16 nt to 36 nt) that are not mapped to rRNA or miRNA. The x axis indicates the size; y axis indicates the reads per million (upper chart) or species per million (lower chart). Three *piwi*$^{1/2}$ replicates are colored in steel blue, cadet blue, and cornflower blue, respectively. Three wild-type replicates are colored in coral, brown, and dark orange, respectively.

(F and G) The base composition of 20–32 nt small RNAs from wild-type (left charts in F and G) and *piwi*$^{1/2}$ (right charts in F and G) that are not mappable to rRNA or miRNA, by reads (F) and by species (G), respectively. The x axis is the position in the 5′ to 3′ direction; y axis is the percentage of base by reads (F) or species (G). Only the first 12 nt are displayed.

See also Tables S1, S2, and S3.

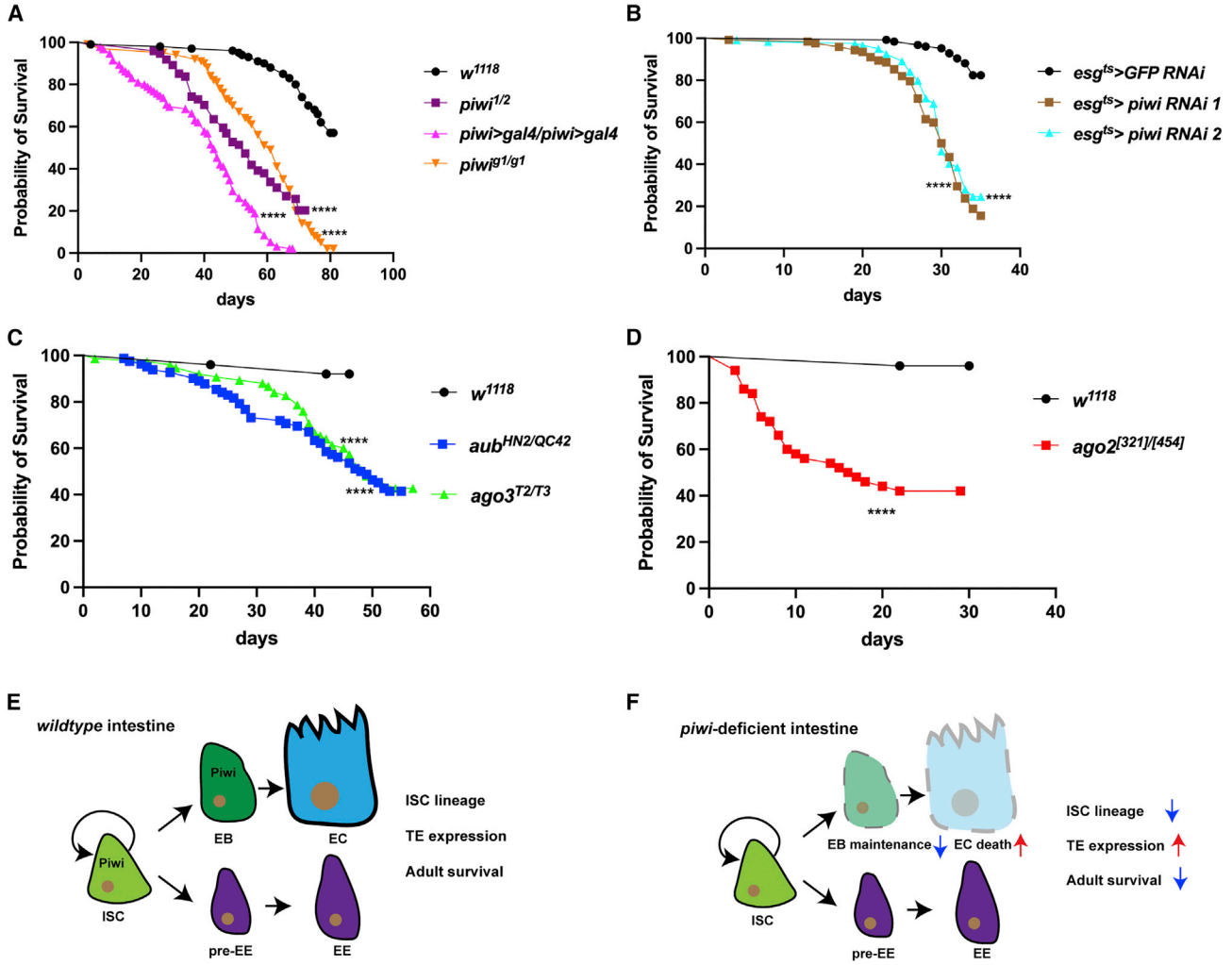

Figure 7. Intestinal Piwi contributes to adult survival

(A) Adult survival assay in the wild-type (black, n = 100), *piwi*$^{1/2}$ (purple, n = 75), *piwi-gal4/piwi-gal4* (magenta, n = 90), and *piwi*$^{g1/g1}$ (orange, n = 100) females at RT. (B) Adult survival assay of the *esg*^{ts}*>GFP RNAi* (black, n = 125), *esg*^{ts}*>piwi RNAi 1* (brown, n = 123), *esg*^{ts}*>piwi RNAi 2* (cyan, n = 119) females at 30°C.

(C and D) Adult survival assay in the control (black, n = 100), *aub*$^{HN2/QC42}$ (blue, n = 75), *ago3*$^{T2/T3}$ (green, n = 90), and *ago2*$^{321/454}$ (red, n = 50) females reared at RT. Statistical significance: Log rank (Mantel-Cox) test. ****p < 0.0001. (E and F) Proposed mode of Piwi function in the homeostatic adult gut.

is responsible for establishing a normal population of ISCs but Piwi expression at the adult stage does not seem to be required for ISC maintenance, in contrast to the continuous requirement of Piwi in GSC maintenance (Cox et al., 1998). In addition, we found that Piwi expression in EBs is required for maintaining the EB population, as EB-specific depletion of Piwi decreased the number of EBs in the gut. This differs from a previous report that Piwi downregulation in EBs did not affect the EB number (Sousa-Victor et al., 2017), an inconsistency that may be due to different *piwi* knockdown experimental designs. Furthermore, by using an ISC lineage tracing system, we found that Piwi has no effect on ISC-to-EE differentiation. Our study indicates that there are two phases of Piwi function in the gut: First, it acts during pre-adult development to ensure the establishment of a normal number of ISCs; second, it acts in the adult ISC lineage to maintain EBs and the survival of the ISC-derived epithelial cells, especially ECs.

Our work represents one of the first studies on the TE-silencing function of Piwi in somatic tissues. We found that the loss of Piwi results in activation of some representative retrotransposons in the gut, which is consistent with a previous report (Sousa-Victor et al., 2017). Furthermore,

we showed that Piwi expression in adult ISCs and EBs is directly responsible for this TE silencing function, without the contribution of maternal Piwi. In addition, we found that some TEs (e.g., *Tabor*, *Rt1a*, *blood*, *412*, *I-element*) are not activated upon *piwi* downregulation in ISCs and EBs, but are drastically upregulated in the *piwi* mutant gut. It is possible that a more efficient Piwi knockdown might be needed to de-repress these TEs in the gut. Alternatively, Piwi might also be expressed in visceral muscle cells of the intestine, as predicated by Flygut-seq data (http://flygutseq.buchonlab.com/data?gene=piwi%0D%0A%0D%0A), to repress these TEs, whereas *esg-gal4* only knocks down *piwi* in the midgut ISCs and EBs. The activation of *Tabor*, *Rt1a*, *blood*, *412*, and *I-element* in the ISCs and EBs alone may not lead to sufficient upregulation of their overall expression in the entire gut.

An interesting finding in our study is that Piwi regulates different TEs in different tissues. In the ovary, Piwi has been implicated in repressing a variety of retrotransposon expressions in both the germline and soma (Wang and Lin, 2021). However, some of activated TEs in the *piwi* mutant ovary are not significantly upregulated either in the $piwi^{1/2}$ mutant gut (*R1A1*) or the head (*412*, *mdg1*, *HMS-Beagle,* and *R1A1*). These observations suggest that different mechanisms may be used to silence TEs in distinct tissues. For example, the linker histone H1 represses TE expression in ovarian somatic cells and larval salivary glands (Lu et al., 2013), whereas the regulation of some other TEs in the soma is both H1 and Piwi-independent (Iwasaki et al., 2016). Furthermore, Ago2 has been reported to repress TE expression in the adult head. Our data, together with a previous report (Siudeja et al., 2021), reveal that the siRNA pathway genes *ago2* and *dcr2* are expressed in the gut to repress TEs. Consistent with this notion, our *gypsy-lacZ* reporter showed high *gypsy* activation in the anterior and posterior midgut, but not in the middle of the midgut. Indeed, *piwi* is predicted to be barely expressed in the middle of the midgut but *ago2* is abundantly transcribed in all subregions of the midgut (http://flygutseq.buchonlab.com/data?gene=ago2%0D%0A%0D%0A). Therefore, it is possible that Ago2 expression in the middle of midgut accounts for *gypsy* silencing and may collaborate with Piwi and other proteins to restrain TE expression in other parts of the midgut.

It is well-known that the Piwi-mediated TE silencing in the germline depends on its associated piRNAs. However, whether *bona fide* piRNAs exist outside the germline remains a mystery. Several groups have attempted to identify piRNAs by small RNA-seq in somatic tissues. They identified a small fraction of 24–28 nt size of putative piRNAs in the head (Ghildiyal et al., 2008; Mirkovic-Hosle and Forstemann, 2014; Yan et al., 2011). However, another group re-analyzed their small RNA-seq data and argued that these putative piRNAs are mostly derived from contaminated gonad RNA during head RNA preparation (van den Beek et al., 2018). A recent study has characterized somatic piRNAs in the adult fat body cells and revealed its canonical role in TE silencing (Jones et al., 2016). Our work, together with that of Sousa-Victor et al. (2017), showed that the depletion of Piwi, a primary piRNA pathway component, activates TE expression in the gut, indicating that the adult gut may harbor somatic piRNA and contribute to TE silencing. However, a recent small RNA-seq effort on the gut did not find any evidence for the presence of piRNA, with most of the gut small RNAs being active siRNAs (Siudeja et al., 2021). Our small RNA-seq data confirmed their finding and suggests that either the expression of gut piRNA is too low to be detected or Piwi has a piRNA-independent function in the gut. Recently, PIWIL1 has been shown to possess a piRNA-independent function in human gastric and pancreatic cancer cells to promote tumorigenesis and metastasis (Shi et al., 2020; Li et al., 2020). Thus, it remains formally possible that Piwi silences TE function in the *Drosophila* gut in a piRNA-independent way.

In addition to TE genes, our mRNA-seq data identified hundreds of differentially expressed protein-coding genes in the $piwi^{1/2}$ mutant gut, implying that Piwi may have multifaced function in the gut. Interestingly, various metabolic genes related to glutathione and carbohydrate metabolism, amino acid and anion transport, glucose homeostasis, and fatty acid metabolism are enriched in our GO analysis. This implies that Piwi may be involved in regulating metabolic processes to maintain gut homeostasis. In addition, gene responses to oxidative stress are also identified in the *piwi* mutant gut. The intracellular level of reactive oxygen species (ROS) has been reported to influence *Drosophila* stem cell activity (Tan et al., 2017; Owusu-Ansah and Banerjee, 2009). An elevated level of ROS promotes the differentiation of both hematopoietic progenitors in the larval lymph gland and GSCs in the adult testis, respectively. Oxidative stress-induced ROS also triggers ISC proliferation and differentiation but a low level of ROS is required to maintain ISCs at the quiescent state (Hochmuth et al., 2011; Biteau et al., 2008; Amcheslavsky et al., 2009). Consequently, Piwi may be involved in regulating ROS levels to control ISC function.

Finally, we found that both *piwi* mutants and *piwi* deficiency in ISCs and EBs shorten adult lifespan, highlighting the importance of intestinal Piwi function in the regulation of adult survival and longevity. We also noticed that Piwi expression in ISCs and EBs is required for normal ISC lineage and gut development. Therefore, it is possible that Piwi-defective ISCs and EBs give rise to abnormal ECs—the major gut cell type for nutrient absorption and metabolism, which in turn cause

dysregulation of genes related to gut development, ultimately affecting longevity.

EXPERIMENTAL PROCEDURES

Resource availability

Corresponding author

Further information and requests for resources and reagents should be directed to the corresponding author, Haifan Lin (haifan.lin@yale.edu)

Materials availability

This study did not generate new unique reagents.

Data and code availability

The mRNA-seq and small RNA-seq data are available at the NCBI SRA under the accession number PRJNA801124. This study did not generate any unique code.

Immunostaining

Five-day-old female adult guts were dissected in PBS (pH 7.4) and immediately transferred and fixed with 4% paraformaldehyde or the fixative as described in Sousa-Victor et al. (2017) for 1 h at room temperature (RT), briefly washed twice with PBST (PBS with 0.1% Triton X-100), and blocked in 5% normal goat serum at RT for 1 h. Primary antibodies were then added and incubated at 4°C overnight. Next day, guts were washed in PBST and incubated with secondary antibodies at RT for 2 h. Finally, guts were stained with DAPI and mounted in Vectashield on the glass slide. Images were acquired by the Leica SP5 confocal and processed with Adobe Photoshop 2020 and Adobe Illustrator 2020.

For DI antibody staining, the detailed procedure was described in Lin et al. (2008). Dissected female guts were fixed in an equal volume of 4% formaldehyde and heptane mix at RT for 15 min. Then the lower layer of fixative was replaced with methanol and gently shaken for 1–2 min. All solutions were subsequently removed and samples were gradually rehydrated in rehydration series (70% MeOH:30% PBST; 50% MeOH:50% PBST; 30% MeOH:70% PBST). From this point onward, immunostaining proceeded as described above.

RT-qPCR

Total RNA was extracted from 20–25 adult female guts with TRIzol (Thermo Fisher Scientific, Cat. No. 15596018). RNA samples were then purified by DNase treatment at 37°C for 30 min using Turbo DNA-free kit (Ambion, Cat. No. AM1907). Next, 1 μg total RNA of each sample was used for 20 μL of cDNA synthesis using the high-capacity cDNA reverse transcription kit (Thermo Fisher Scientific, Cat. No. 4368814). Finally, transcripts of interest were amplified using iTaq Universal SYBR Green (BioRad, Cat. No. 1725121) on the BioRad CFX96/384 Real-Time machine. All experiments were analyzed in at least three biological triplicates and the measured mRNA expression levels were normalized relative to those of *RpL32*. Primer sequences are listed in the Table S4.

Northern blotting

Briefly, 5 μg of total RNA was loaded and run on 1% denatured formaldehyde agarose gel and then transferred overnight to Amersham Hybond N+ nylon membrane (GE Healthcare, Cat. No. RPN303T) in 20x SSC buffer at RT. Next day, the membrane was stained by 0.02% methylene blue dye to examine transfer efficiency. Then, the dried membrane was placed between two pieces of 3MM paper and baked for 2 h at 80°C, followed by UV irradiation (0.15 J/sq.cm) to cross-link RNA to the membrane. Finally, the filter was hybridized overnight by radiolabeled probes at 68°C and then scanned in a Typhoon scanner after washing with 2x SSC, 0.1% SDS and 0.2x SSC, 0.1% SDS buffer, respectively. The ^{32}P-labeled RNA probes were synthesized by using the HiScribe T7 High Yield RNA Synthesis Kit (NEB, Cat. No. E2040) according to the manufacturer's instructions. The primer sequence for RNA probes synthesis are listed in Table S4.

Statistical analysis

Statistical significance was assessed using either unpaired Student's t tests in pairwise comparisons or multiple t tests in groups, as shown in related figures via the GraphPad Prism 9 software.

SUPPLEMENTAL INFORMATION

Supplemental information can be found online at https://doi.org/10.1016/j.stemcr.2023.01.001.

AUTHOR CONTRIBUTIONS

Conceptualization: X.T. and H.L.; experimental investigation: X.T., H.Q.; data analysis: X.T., H.Q., and H.L.; bioinformatic analysis: N.L.; original draft: X.T. and H.L.; revision: X.T., H.L., N.L., and H.Q.

ACKNOWLEDGMENTS

We thank Dr. Phillip Zamore for anti-Aub and Anti-Ago3 antibodies; Dr. Astrid Haase for the *piwi-gal4* line; the Bloomington Stock Center and Vienna *Drosophila* Resource Center for other fly lines; Dr. Nils Neuenkirchen, Jiaying Chen, Tianshu Liu, Yuqi Wang for valuable comments on the manuscript; Yale Stem Cell Center Genomics core and Yale Center for Genome Analysis core for high throughput sequencing; and Yale Stem Cell Center Imaging core for confocal service. This work was funded by the Michael Vranos Family Foundation and a gift from Luye Pharmaceuticals to H.L.

CONFLICT OF INTERESTS

The authors declare no competing interests.

Received: February 8, 2022
Revised: December 28, 2022
Accepted: January 3, 2023
Published: February 2, 2023

REFERENCES

Akkouche, A., Mugat, B., Barckmann, B., Varela-Chavez, C., Li, B., Raffel, R., Pélisson, A., and Chambeyron, S. (2017). Piwi is required during Drosophila embryogenesis to license dual-strand piRNA clusters for transposon repression in adult ovaries. Mol. Cell *66*, 411–419.e4. https://doi.org/10.1016/j.molcel.2017.03.017.

Amcheslavsky, A., Jiang, J., and Ip, Y.T. (2009). Tissue damage-induced intestinal stem cell division in Drosophila. Cell Stem Cell *4*, 49–61. https://doi.org/10.1016/j.stem.2008.10.016.

Apidianakis, Y., and Rahme, L.G. (2011). Drosophila melanogaster as a model for human intestinal infection and pathology. Dis. Model. Mech. *4*, 21–30. https://doi.org/10.1242/dmm.003970.

Biteau, B., Hochmuth, C.E., and Jasper, H. (2008). JNK activity in somatic stem cells causes loss of tissue homeostasis in the aging Drosophila gut. Cell Stem Cell *3*, 442–455. https://doi.org/10.1016/j.stem.2008.07.024.

Brower-Toland, B., Findley, S.D., Jiang, L., Liu, L., Yin, H., Dus, M., Zhou, P., Elgin, S.C.R., and Lin, H. (2007). Drosophila PIWI associates with chromatin and interacts directly with HP1a. Genes Dev. *21*, 2300–2311. https://doi.org/10.1101/gad.1564307.

Buchon, N., Osman, D., David, F.P.A., Fang, H.Y., Boquete, J.P., Deplancke, B., and Lemaitre, B. (2013). Morphological and molecular characterization of adult midgut compartmentalization in Drosophila. Cell Rep. *3*, 1725–1738. https://doi.org/10.1016/j.celrep.2013.04.001.

Chung, W.J., Okamura, K., Martin, R., and Lai, E.C. (2008). Endogenous RNA interference provides a somatic defense against Drosophila transposons. Curr. Biol. *18*, 795–802. https://doi.org/10.1016/j.cub.2008.05.006.

Cox, D.N., Chao, A., Baker, J., Chang, L., Qiao, D., and Lin, H. (1998). A novel class of evolutionarily conserved genes defined by *piwi* are essential for stem cell self-renewal. Genes Dev *12*, 3715–3727.

Czech, B., Malone, C.D., Zhou, R., Stark, A., Schlingeheyde, C., Dus, M., Perrimon, N., Kellis, M., Wohlschlegel, J.A., Sachidanandam, R., et al. (2008). An endogenous small interfering RNA pathway in Drosophila. Nature *453*, 798–802. https://doi.org/10.1038/nature07007.

Elmaghraby, M.F., Andersen, P.R., Pühringer, F., Hohmann, U., Meixner, K., Lendl, T., Tirian, L., and Brennecke, J. (2019). A heterochromatin-specific RNA export pathway facilitates piRNA production. Cell *178*, 964–979.e20. https://doi.org/10.1016/j.cell.2019.07.007.

Furriols, M., and Bray, S. (2001). A model Notch response element detects Suppressor of Hairless-dependent molecular switch. Curr. Biol. *11*, 60–64. https://doi.org/10.1016/S0960-9822(00)00044-0.

Ghildiyal, M., Seitz, H., Horwich, M.D., Li, C., Du, T., Lee, S., Xu, J., Kittler, E.L.W., Zapp, M.L., Weng, Z., and Zamore, P.D. (2008). Endogenous siRNAs derived from transposons and mRNAs in Drosophila somatic cells. Science *320*, 1077–1081. https://doi.org/10.1126/science.1157396.

Gonzalez, L.E., Tang, X., and Lin, H. (2021). Maternal Piwi regulates primordial germ cell development to ensure the fertility of female progeny in Drosophila. Genetics *219*, iyab091. https://doi.org/10.1093/genetics/iyab091.

Gu, T., and Elgin, S.C.R. (2013). Maternal depletion of Piwi, a component of the RNAi system, impacts heterochromatin formation in Drosophila. PLoS Genet. *9*, e1003780. https://doi.org/10.1371/journal.pgen.1003780.

Hochmuth, C.E., Biteau, B., Bohmann, D., and Jasper, H. (2011). Redox regulation by Keap1 and Nrf2 controls intestinal stem cell proliferation in Drosophila. Cell Stem Cell *8*, 188–199. https://doi.org/10.1016/j.stem.2010.12.006.

Iwasaki, Y.W., Murano, K., Ishizu, H., Shibuya, A., Iyoda, Y., Siomi, M.C., Siomi, H., and Saito, K. (2016). Piwi modulates chromatin accessibility by regulating multiple factors including histone H1 to repress transposons. Mol. Cell *63*, 408–419. https://doi.org/10.1016/j.molcel.2016.06.008.

Jiang, H., Patel, P.H., Kohlmaier, A., Grenley, M.O., Mcewen, D.G., and Edgar, B.A. (2009). Cytokine/jak/stat signaling mediates regeneration and homeostasis in the Drosophila midgut. Cell *137*, 1343–1355. https://doi.org/10.1016/j.cell.2009.05.014.

Jones, B.C., Wood, J.G., Chang, C., Tam, A.D., Franklin, M.J., Siegel, E.R., and Helfand, S.L. (2016). A somatic piRNA pathway in the Drosophila fat body ensures metabolic homeostasis and normal lifespan. Nat. Commun. *7*, 13856. https://doi.org/10.1038/Ncomms13856.

Kawamura, Y., Saito, K., Kin, T., Ono, Y., Asai, K., Sunohara, T., Okada, T.N., Siomi, M.C., and Siomi, H. (2008). Drosophila endogenous small RNAs bind to Argonaute 2 in somatic cells. Nature *453*, 793–797. https://doi.org/10.1038/nature06938.

Lee, T., and Luo, L. (2001). Mosaic analysis with a repressible cell marker (MARCM) for Drosophila neural development. Trends Neurosci. *24*, 251–254. https://doi.org/10.1016/S0166-2236(00)01791-4.

Lemaitre, B., and Miguel-Aliaga, I. (2013). The digestive tract of Drosophila melanogaster. Annu. Rev. Genet. *47*, 377–404. https://doi.org/10.1146/annurev-genet-111212-133343.

Li, C., Vagin, V.V., Lee, S., Xu, J., Ma, S., Xi, H., Seitz, H., Horwich, M.D., Syrzycka, M., Honda, B.M., et al. (2009). Collapse of germline piRNAs in the absence of Argonaute3 reveals somatic piRNAs in flies. Cell *137*, 509–521. https://doi.org/10.1016/j.cell.2009.04.027.

Li, F., Yuan, P., Rao, M., Jin, C.H., Tang, W., Rong, Y.F., Hu, Y.P., Zhang, F., Wei, T., Yin, Q., et al. (2020). piRNA-independent function of PIWIL1 as a co-activator for anaphase promoting complex/cyclosome to drive pancreatic cancer metastasis. Nat. Cell Biol. *22*, 425–438. https://doi.org/10.1038/s41556-020-0486-z.

Lin, G., Xu, N., and Xi, R. (2008). Paracrine Wingless signalling controls self-renewal of Drosophila intestinal stem cells. Nature *455*, 1119–1123. https://doi.org/10.1038/nature07329.

Lu, X., Wontakal, S.N., Kavi, H., Kim, B.J., Guzzardo, P.M., Emelyanov, A.V., Xu, N., Hannon, G.J., Zavadil, J., Fyodorov, D.V., and Skoultchi, A.I. (2013). Drosophila H1 regulates the genetic activity of heterochromatin by recruitment of su(var)3-9. Science *340*, 78–81. https://doi.org/10.1126/science.1234654.

Micchelli, C.A., and Perrimon, N. (2006). Evidence that stem cells reside in the adult Drosophila midgut epithelium. Nature *439*, 475–479. https://doi.org/10.1038/nature04371.

Mirkovic-Hösle, M., and Förstemann, K. (2014). Transposon defense by endo-siRNAs, piRNAs and somatic pilRNAs in Drosophila: contributions of Loqs-PD and R2D2. PLoS One *9*, e84994. https://doi.org/10.1371/journal.pone.0084994.

Ohlstein, B., and Spradling, A. (2006). The adult Drosophila posterior midgut is maintained by pluripotent stem cells. Nature *439*, 470–474. https://doi.org/10.1038/nature04333.

Owusu-Ansah, E., and Banerjee, U. (2009). Reactive oxygen species prime Drosophila haematopoietic progenitors for differentiation. Nature *461*, 537–541. https://doi.org/10.1038/nature08313.

Pal-Bhadra, M., Leibovitch, B.A., Gandhi, S.G., Chikka, M.R., Bhadra, U., Birchler, J.A., and Elgin, S.C.R. (2004). Heterochromatic silencing and HP1 localization in Drosophila are dependent on the RNAi machinery. Science *303*, 669–672. https://doi.org/10.1126/science.1092653.

Ramat, A., and Simonelig, M. (2021). Functions of PIWI proteins in gene regulation: new arrows added to the piRNA quiver. Trends Genet. *37*, 188–200. https://doi.org/10.1016/j.tig.2020.08.011.

Ross, R.J., Weiner, M.M., and Lin, H. (2014). PIWI proteins and PIWI-interacting RNAs in the soma. Nature *505*, 353–359. https://doi.org/10.1038/nature12987.

Senti, K.A., Jurczak, D., Sachidanandam, R., and Brennecke, J. (2015). piRNA-guided slicing of transposon transcripts enforces their transcriptional silencing via specifying the nuclear piRNA repertoire. Genes Dev. *29*, 1747–1762. https://doi.org/10.1101/gad.267252.115.

Shi, S., Yang, Z.Z., Liu, S., Yang, F., and Lin, H. (2020). PIWIL1 promotes gastric cancer via a piRNA-independent mechanism. Proc. Natl. Acad. Sci. USA *117*, 22390–22401. https://doi.org/10.1073/pnas.2008724117.

Sienski, G., Batki, J., Senti, K.A., Dönertas, D., Tirian, L., Meixner, K., and Brennecke, J. (2015). Silencio/CG9754 connects the Piwi-piRNA complex to the cellular heterochromatin machinery. Genes Dev. *29*, 2258–2271. https://doi.org/10.1101/gad.271908.115.

Siudeja, K., Van Den Beek, M., Riddiford, N., Boumard, B., Wurmser, A., Stefanutti, M., Lameiras, S., and Bardin, A.J. (2021). Unraveling the features of somatic transposition in the Drosophila intestine. EMBO J. *40*, e106388. https://doi.org/10.15252/embj.2020106388.

Sousa-Victor, P., Ayyaz, A., Hayashi, R., Qi, Y., Madden, D.T., Lunyak, V.V., and Jasper, H. (2017). Piwi is required to limit exhaustion of aging somatic stem cells. Cell Rep. *20*, 2527–2537. https://doi.org/10.1016/j.celrep.2017.08.059.

Stein, C.B., Genzor, P., Mitra, S., Elchert, A.R., Ipsaro, J.J., Benner, L., Sobti, S., Su, Y., Hammell, M., Joshua-Tor, L., and Haase, A.D. (2019). Decoding the 5′ nucleotide bias of PIWI-interacting RNAs. Nat. Commun. *10*, 828. https://doi.org/10.1038/s41467-019-08803-z.

Tan, S.W.S., Lee, Q.Y., Wong, B.S.E., Cai, Y., and Baeg, G.H. (2017). Redox homeostasis plays important roles in the maintenance of the Drosophila testis germline stem cells. Stem Cell Rep. *9*, 342–354. https://doi.org/10.1016/j.stemcr.2017.05.034.

Van Den Beek, M., Da Silva, B., Pouch, J., Ali Chaouche, M.E.A., Carré, C., and Antoniewski, C. (2018). Dual-layer transposon repression in heads of Drosophila melanogaster. RNA *24*, 1749–1760. https://doi.org/10.1261/rna.067173.118.

Wang, C., and Lin, H. (2021). Roles of piRNAs in transposon and pseudogene regulation of germline mRNAs and lncRNAs. Genome Biol. *22*, 27. https://doi.org/10.1186/s13059-020-02221-x.

Wang, L., Zeng, X., Ryoo, H.D., and Jasper, H. (2014). Integration of UPRER and oxidative stress signaling in the control of intestinal stem cell proliferation. PLoS Genet. *10*, e1004568. https://doi.org/10.1371/journal.pgen.1004568.

Yamashiro, H., and Siomi, M.C. (2018). PIWI-interacting RNA in Drosophila: biogenesis, transposon regulation, and beyond. Chem. Rev. *118*, 4404–4421. https://doi.org/10.1021/acs.chemrev.7b00393.

Yan, Z., Hu, H.Y., Jiang, X., Maierhofer, V., Neb, E., He, L., Hu, Y., Hu, H., Li, N., Chen, W., and Khaitovich, P. (2011). Widespread expression of piRNA-like molecules in somatic tissues. Nucleic Acids Res. *39*, 6596–6607. https://doi.org/10.1093/nar/gkr298.

Yin, H., and Lin, H. (2007). An epigenetic activation role of Piwi and a Piwi-associated piRNA in Drosophila melanogaster. Nature *450*, 304–308. https://doi.org/10.1038/nature06263.

Yu, Y., Gu, J., Jin, Y., Luo, Y., Preall, J.B., Ma, J., Czech, B., and Hannon, G.J. (2015). Panoramix enforces piRNA-dependent cotranscriptional silencing. Science *350*, 339–342. https://doi.org/10.1126/science.aab0700.